JOURNAL OF OPTOELECTRONICS AND ADVANCED MATERIALS, Vol. 12, No. 6, June 2010, p. 1433 - 1441

Morphology and optical properties of Mg doped GaN nanowires in dependence of growth temperature

F. LIMBACH*, E. O. SCHÄFER-NOLTE, R. CATERINO, T. GOTSCHKE, T. STOICA, E. SUTTER[a], R. CALARCO
Institute of Bio- and Nanosystems (IBN-1), Research Centre Jülich GmbH, 52425 Jülich, Germany, and JARA-FIT Fundamentals of Future Information Technology
[a]*Center for Functional Nanomaterials, Brookhaven National Laboratory, Upton, New York 11973*

The influence of the substrate temperature and Mg doping on the morphological and optical properties of catalyst-free GaN nanowires grown by plasma-assisted molecular beam epitaxy on Si(111) has been investigated in a large temperature range between 665°C and 785°C. The density and wire sizes in Mg-doped nanowires are found to change with substrate temperature in a similar way as undoped nanowires. Between 725 °C and 785 °C a trimodal size distribution and an increase of the wire density from 5.0×10^9 cm^{-2} to 9.5×10^9 cm^{-2} were observed. Transmission electron microscopy indicates that the upper parts of the nanowires are free of structural defects. Raman spectroscopy measurements confirm a high crystalline quality of doped wires, with a line width of the E_2^H of 3.3 cm^{-1} for samples grown at T_S=785 °C. Photoluminescence measurements show a strong influence of Mg on the emission properties, namely the increase of the donor-acceptor pair emission and its phonon replicas.

(Received April 30, 2010; accepted June 16, 2010)

Keywords: GaN, MG-doping, Nanowire, MBE, Photo-luminescence

1. Introduction

GaN is one of the most important III-V semiconductor compounds in today's electronics and optoelectronics. Its tunable band gap, when alloyed with In and Al, as well as its thermal, chemical and mechanical stability make it a very versatile material. Thin films of GaN have been already used successfully in different kinds of electronic and optoelectronic devices [1]. However issues like reduction of the high dislocation density, caused by a large lattice mismatch to the substrate, still need to be solved. In this respect self-assembled GaN nanowires (NWs) grown by plasma-assisted molecular beam epitaxy (PAMBE) represent an interesting alternative, as they show high crystal quality, low defect densities and strong luminescence [1-14].

An important step in the development of GaN based nanodevices is p-type doping. Mg is widely used as a p-type dopant for epilayers and has been subject of a number of studies using photoluminescence (PL) [15]. It is of importance to achieve doping control for GaN NWs as well, in order to use them in electronic or optoelectronic devices [16]. The impact of Mg doping on the nanowire morphology was already demonstrated and an increased lateral growth upon increasing Mg supply was reported [17,18]. The influence of Mg on the optical properties of GaN NWs at a given substrate temperature was also investigated [19,20].

In this paper, we report on the effect of the growth temperature (T_S) on both the morphology and optical properties of Mg-doped and undoped GaN NWs. A low Mg doping level was chosen in order to minimize the impact of doping on the NW morphology.

2. Experimental details

GaN NWs were grown on Si(111) substrates in nitrogen rich conditions (Ga/N << 1) by PAMBE without any metal catalyst. The silicon substrates have been cleaned before epitaxy by a standard ex-situ chemical cleaning procedure and by in situ annealing in ultra-high vacuum at 925 °C for 15 min, in order to obtain an oxygen-free surface with a 7×7 reconstruction. The GaN NWs were doped with Mg (the cell temperature was 185°C resulting in beam equivalent pressure (BEP_{Mg}) = 1.0×10^{-9} mbar) using identical growth parameters as for undoped GaN NWs: $BEP_{Ga} = 2.4 \times 10^{-8}$ mbar, RF-power P_{RF} =500 W, a nitrogen flow rate of 4 sccm and a growth duration of 2h. The influence of the substrate temperature on the morphology and optical properties was investigated for samples grown at different T_S between 665 °C and 785 °C.

Investigation of the morphology of the NWs was carried out in a Zeiss Leo1550 scanning electron microscope (SEM) and a JEOL-3000F transmission electron microscope (TEM). μ-Raman scattering measurements were performed in backscattering geometry on freestanding NWs (FSNWs) dispersed on glass susbstrates in order to eliminate the strong signal of the c-Si substrate of the as grown samples. The 514 nm laser line of an Ar^+ gas laser was used as excitation source. The laser beam was focused onto the sample by a 100x

objective (N.A. 0.95). The backscattered light was guided to a triple grating spectrometer (Dilor XY500) and finally detected with a resolution of 0.022 nm by a CCD camera. PL measurements were performed using the 325nm line of a Cd-He Laser as an excitation source. The as grown samples were mounted in a liquid He cooled cryostat. Spectral analysis of the signal was carried out with a Czerny-Turner monocromator (SPEX 1702, 0.75m focal length) and detected with a CCD camera.

3. Results and discussion

SEM side view images of the as grown samples were used to determine diameter and length distributions. Top view images were used to evaluate the density of the nanowires. In Fig. 1 the SEM side view images are presented for four of the Mg doped samples. The NW samples exhibit roughly four distinguished morphology regimes. At lower growth temperatures (665 °C to 685 °C) an almost compact layer made up of coalesced NWs with a height of approximately 570 nm is formed. Out of this layer a few rather long wires emerge (Fig. 1a). In the intermediate temperature range 725 °C to 755 °C a trimodal NW growth mode is observed. The length of most wires was found to be around 600 nm with an average diameter of about 60 nm. A number of thin NWs are observed that exhibit a much higher aspect ratio.

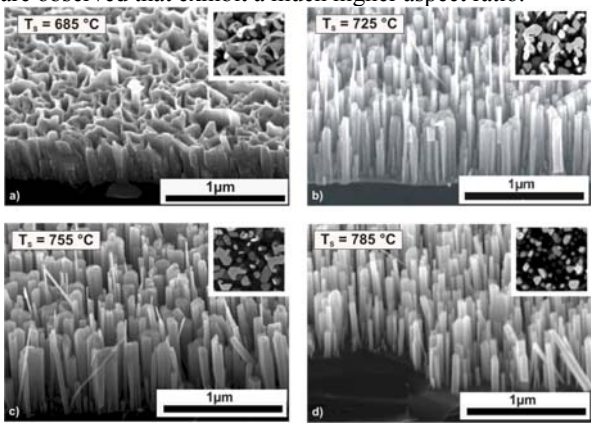

Fig.1. a) – d) SEM side view images (tilt = 45°) of GaN:Mg NWs grown at different temperatures T_S. The insets are top view SEM images of the corresponding samples at the same magnification containing 26, 32 and 46 wires for the insets b), c) and d) respectively. The number of wires in the inset of a) cannot be evaluated as it is an almost compact layer.

A third class of NWs is present with wires that have a length below 400 nm and small diameters below 40 nm. This can be seen in the histogram of Fig. 2a where the peak around 600 nm in length represents the first class of wires, while the counts at 850 nm and above originate from the wires with an increased aspect ratio. At elevated T_S (785 °C) nanowires are well separated and show a narrow quasi-cylindrical shape. At even higher temperatures a significant decrease in diameter, length, as well as density (results not shown here) are observed, due to Ga desorption as well as GaN decomposition [21].

The average length for each class of the trimodal nanowire distribution has been calculated for all the samples (shown in Fig. 2a). The length of the wires in the different classes is slightly decreasing as a function of substrate temperature as can be seen in Fig. 3a. This behavior might be explained by the increase of the Ga desorption rate at higher growth temperatures.

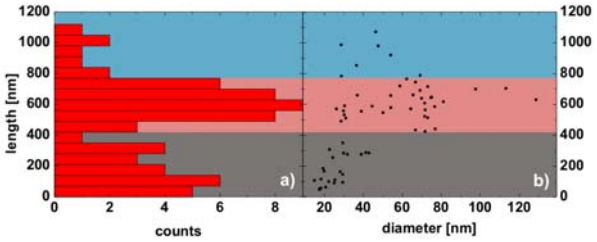

Fig. 2. a) Histogram of the length of NWs found for T_S = 725 °C; b) Diameter and length correlation for the same data set. The color code indicates the trimodal distribution.

We can identify a suitable temperature window (725 °C - 785 °C) for the growth of Mg doped GaN NW, using as the only criterion the best quasi-cylindrical morphology. The lower limit of the growth temperature for the used growth parameters is defined by the formation of an almost compact layer at $T_S \leq 725$ °C, and the upper limit is determined by the Ga desorption rate which becomes the dominating process at $T_S = 800$ °C.

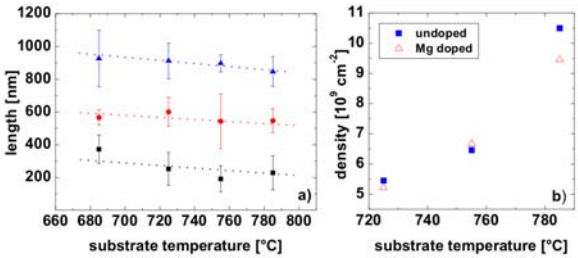

Fig. 3. a) Average length for each wire class as a function of temperature. The error represents the standard deviation, the dashed lines are guides to the eye; b) Density of wires as a function of substrate temperature. The data are calculated from SEM images showing an area of 4 µm^2.

The NW density increases with T_S within the temperature range 725°C – 685°C, as can be observed in the top view SEM images shown as insets in Fig. 1a-1c and is numerically shown by the statistical data in Fig. 3b calculated from SEM images of 4.0 µm^2 areas.The density amounts to 5.5×10^9 cm^{-2} at T_S = 725 °C, whereas it increases to 9.5×10^9 cm^{-2} at T_S = 785 °C. This effect is due to a reduction of the NW coalescence at higher temperatures because of the enhanced diffusion of Ga

adatoms toward the NW top, and results in an reduction in lateral growth rate in respect to the vertical one [8]. While at lower temperatures the difference in density between doped and undoped sample is negligible, it is more pronounced at T_S = 785 °C and is caused by a stronger tendency of coalescence for doped wires. Thus at this high temperature not only the best morphology but also the highest NW density can be reached.

In order to investigate the effect of coalescence on the morphology of the GaN:Mg NWs TEM measurements were performed. The TEM image in Fig. 4 shows the bottom of a typical Mg-doped nanowire. The NWs show few structural defects, those defects that are observed are induced by coalescence of wires and are present close to the base of the NWs, but once the coalescence is complete (within a 20-30 nm) wires grow without visible morphological defects [22]. Stacking faults or zincblende type insertions as reported in the case of higher Mg supply [18] were not observed in our samples.

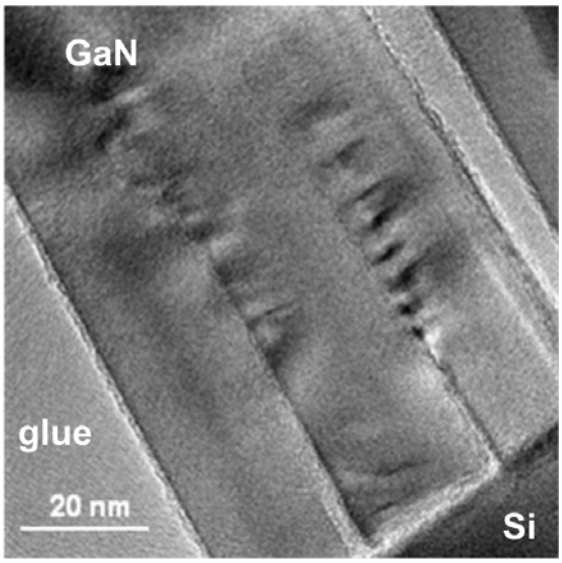

Fig. 4. TEM image of the bottom part of a Mg-doped GaN NW. The coalescence of formerly three wires is completed within a few 10 nm and the strain caused by the interfaces is relaxed at a similar length scale.

Raman spectra for Mg doped FSNWs are shown in Fig. 5a together with peak positions of different scattering modes in GaN taken from literature [20]. Intense and sharp E_2^H peak (FWHM 3.15 cm^{-1} - 4.15 cm^{-1}) can be seen in all spectra, as well as a strong A_1(TO) peak. With increasing growth temperature A_1(TO) shows a decreasing peak intensity with respect to E_2^H, its line shape becomes more asymmetric with a tail at the high wavenumber side. E_1(TO) is weakly pronounced as a shoulder of the E_2^H peak.

Besides these phonon modes of GaN two additional broad peaks of unclear origin can be observed within the range 400 – 500 cm^{-1}. The peak around 420 cm^{-1} might be attributed to a vacancy related defect mode [23,24]. Furthermore, a weak Si Raman signal probably originating from Si particles that have remained attached to the nanowire cluster despite its removal from the substrate is present in the spectrum of FSNW from the sample grown at 785 °C (peak at 520 cm^{-1}).

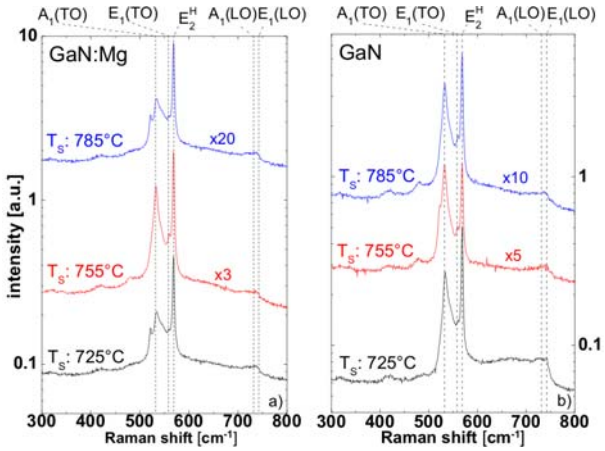

Fig. 5. Raman graphs of (a) Mg-doped and (b) undoped GaN NWs grown at three different temperatures. The positions of the Raman peaks shown here as vertical dotted lines were taken from Ref. [20].

The Raman spectra of the undoped reference samples are given in Fig. 5b. They show the same characteristics as the spectra of the Mg doped samples described above. Additionally a broad peak can be found close to the position of the LO modes. However, quantitative differences between Raman spectra of doped and undoped NWs can be detected. The A_1(TO) peak intensity normalized to the E_2^H mode is reduced for the doped sample compared to their undoped counterparts. This is due to the polar character of the A_1(TO) mode, therefore it is more sensitive to changes of the carrier concentration. The sharpness of the E_2^H which gives information about the crystalline quality is enhanced by Mg doping as will be discussed later on associated with the PL results.

Harima et. al. [23] studied Mg doped GaN films and found significant changes in the Raman spectra for increasing hole concentrations. They observed a low frequency (< 300 cm^{-1}) continuum band arising from light scattering of free holes and a vibrational mode at 657 cm^{-1}, which was attributed to a Mg-N vibration. The fact that none of these features could be observed in the spectra of our Mg doped NWs is a confirmation that the Mg concentration in these nanowires is low. Also in energy dispersive x-ray spectra (EDS) acquired from isolated NWs in a HRTEM with a 10 nm spot size, Mg signal was lower than the detection limit.

The PL spectra for doped and undoped GaN NWs grown under the same conditions at 785°C, 755 °C and 725°C substrate temperature are shown in Fig. 6a. The major difference that can be observed between Mg doped and undoped NWs is a strong enhancement of the UV

luminescence band between 3.00 eV and 3.26 eV, which is assigned to donor-acceptor pair (DAP) transitions and their phonon replica (red shifted by 92meV) [15,19].

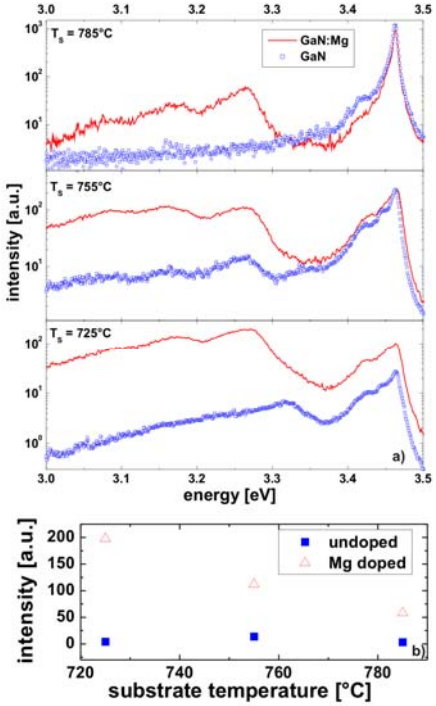

Fig. 6. a) PL spectra of doped NW samples (red lines) and undoped NW samples (blue squares) at different substrate temperatures; b) PL intensity at 3.26 eV for samples displayed in (a).

In the PL signal of the samples grown at different substrate temperatures the relative intensity of the UV band in respect to the near band edge peak is increasing as the substrate temperature is decreasing. Since undoped GaN nanowires show an unintentionally n-type doping [25] the increase in the UV-band ascribed to a DAP transition is most likely due to an enhanced concentration of acceptor states caused by the Mg dopant. As pointed out in Ref. [15] the PL spectra within the DAP range have also a contribution from a broad emission (peak at 2.95 eV) associated with defects. This broad peak is increased at lower deposition temperatures and partially covers the DAP contribution.

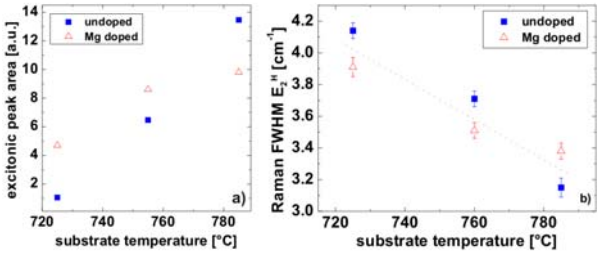

Fig. 7. a) Integrated signal of the excitonic peak of doped and undoped NW samples between 3.37 eV and 3.55 eV at different substrate temperatures; b) FWHM of the E_2^H of doped and undoped NW samples at different substrate temperatures, the dashed line is a guide to the eye.

For a given temperature T_S, the intensity of the onset peak of the UV-band at 3.26 eV in respect to the excitonic peak is significantly modified by Mg incorporation into the wires and can be used as a measure of Mg incorporation. However, the evaluation procedure proposed here using the DAP peak cannot be used to compare samples obtained at different Ts, because additional effects like for example the temperature dependence of the unintentional donor state formation and also the defect band at 2.95 eV effect the PL spectra in the DAP energy range. The luminescence intensity of the UV band as a whole in doped wires increases for lower T_S (see Fig. 6b). Its relative intensity compared to the near band edge peak of both doped and undoped NWs behaves likewise. The reduction in T_S causes a broadening of the exitonic peak (at 3.4 eV, Fig. 6a) and a decrease in total luminescence efficiency (Fig. 7a) due to degradation in material quality. As we can see from Fig. 7a, the efficiency of the excitonic emission is increased by Mg incorporation at low temperatures. On the contrary, at high deposition temperature, the efficiency is reduced in Mg doped samples. We can conclude that apparently the crystal quality of the NWs is improved at low deposition temperature by Mg doping and it is reduced for high temperatures. The additional disorder due to doping could explain the reduction of the crystal quality at high temperature. At low temperatures, as discussed above, Mg doping results in a stronger coalescence, and thus many bulk-like single crystal columns with bigger diameter are formed. The increase of the crystal size, which has a benefit for the optical efficiency, may overcome the effect of the doping-induced disorder. These results are in agreement with Raman measurements. The FWHM of the E_2^H Raman peak decreases with T_S for both doped and undoped NWs, showing an increase of the crystal quality at higher temperatures (Fig. 7b, data extracted from Fig. 5). Similarly to the PL measurements, Mg incorporation effect on FWHM of the E_2^H Raman peak has a non-monotonic dependence (Fig. 7b), resulting at low temperatures in lower FWHM values for doped samples, which corresponds to a better crystal quality, while at higher temperature a reverse effect is observed.

4. Conclusions

In conclusion, we have investigated the effect of the substrate temperature on the optical and morphological properties of Mg doped GaN NWs in comparison to their undoped counterparts. Mg at low doping levels can be incorporated into catalyst-free MBE grown GaN NWs, preserving the columnar morphology within the growth temperature range 725°C-785°C. A trimodal statistical distribution of the NW length was observed and discussed. The NW coalescence takes place close to the NW base for

Mg doped samples, and its probability increases at low temperatures resulting in a decrease of the NW density. Low Mg doping used in this paper leaves Raman spectra only slightly modified while influencing considerably PL emission. PL shows clearly the Mg incorporation into the NWs by an order of magnitude increase of the DAP emission. This sensitivity can be used for the detection of the Mg doping, and the ratio of DAP and excitonic peak intensities might offer a comparative evaluation at a specific temperature, for low doping levels.

Acknowledgements

The authors gratefully acknowledge fruitful discussions and suggestions by Prof. D. Grützmacher. The authors wish to thank also K. H. Deussen for technical support. This work was financially supported by the German Ministry of Education and Research project "QPENS". It was performed in part under the auspices of the U.S. Department of Energy, under contract No. DE-AC02-98CH1-886.

References

[1] H. Morkoç, Handbook of Nitride Semiconductors and Devices, Volume 3: GaN-based Optical and Electronical Devices (Weinheim, Germany, 2009).
[2] E. Calleja, M. A. Sánchez-Garciá, F. J. Sánchez, F. Calle, F. B. Naranjo, E. Muñoz, U. Jahn, K. Ploog, Phys. Rev. B **62**, 16826 (2000).
[3] R. Meijers, T. Richter, R. Calarco, T. Stoica, H. P. Bochem, M. Marso and H. Lüth, J. Cryst. Growth **289**, 381 (2006).
[4] N. Thillosen, K. Sebald, H. Hardtdegen, R. Meijers, R. Calarco, S. Montanari, N. Kaluza, J. Gutowski, H. Luth, Nano Lett. **6,** 704 (2006)
[5] L. Robins, K. A. Bertness, J. M. Barker, N. A. Sanford, J. B. Schlager, J. Appl. Phys. **101,** 11 113505 (2007)
[6] L. Cerutti, J. Ristic, S. Fernandez-Garrido, E. Calleja, A. Trampert, K. H. Ploog, S. Lazic, J. M. Calleja, Appl. Phys. Lett. **88,** 213114 (2006)
[7] J. Renard, R. Songmuang, C. Bougerol, B. Daudin, B. Gayral, Nano Lett. **8,** 2092 (2008)
[8] R. Calarco, R. J. Meijers, R. K. Debnath, T. Stoica, E. Sutter, H. Lüth, Nano Lett. **7**, 2248 (2007)
[9] T. Stoica, E. Sutter, R. Meijers, R. K. Debnath, R. Calarco, H. Lüth, Small **4**, 751 (2008).
[10] K. Goodman, K. Wang, X. Luo, J. Simon, T. Kosel, D. Jena, Mater. Res. Soc. Symp. Proc. **1080**, 1080-O08-04 (2008)
[11] R. K. Debnath, R. Meijers, T. Richter, T. Stoica, R. Calarco, H. Lüth, Appl. Phys. Lett. **90**, 123117 (2007)
[12] R. Calarco, M. Marso, Appl. Phys. A **87**, 499 (2007).
[13] A. G. Milekhin, R. Meijers, T. Richter, R. Calarco, S. Montanari, H. Lüth, B. A. Paez Sierra, D. R. T. Zahn, J. Phys.: Condens. Matter **18**, 5825 (2006)
[14] A. G. Milekhin, R. Meijers, T. Richter, R. Calarco, H. Lüth, D. R. T. Zahn, Phys. Status Solidi C **3**, 2065 (2006)
[15] M.A. Reshchikov, H. Morkoç, J. Appl. Phys. **97**, 061301 (2005)
[16] K. Kishino, A. Kikuchi, H. Sekiguchi, S. Ishizawa; Proceedings of the society of photo-optical instrumentation engineers (SPIE) **6473,** T4730 (2007)
[17] F. Furtmayr, M. Vielemeyer, M. Stutzmann, J. Arbiol, S. Estrade, F. Peiro, J. R. Morante, M. Eickhoff, J. Appl. Phys. **104,** 034309 (2008)
[18] J. Arbiol, S. Estrade, J. D. Prades, A. Cirera, F. Furtmayr, C. Stark, A. Laufer, M. Stutzmann, M. Eickhoff, M. H. Gass, A. L. Bleloch, F. Peiro, J. R. Morante, Nanotechnology **20**, 145704 (2009)
[19] F. Furtmayr, M. Vielemeyer, M. Stutzmann, A. Laufer, B. K. Meyer, M. Eickhoff, J. Appl. Phys. **104**, 074309 (2008)
[20] Y. Park, J. Na, R. Taylor, Nanotechnology **17**, 913-916 (2006)
[21] S. Fernández-Garrido, G. Kolbmüller, E. Calleja, J. S. Speck, J. Appl. Phys. **104**, 033541 (2008)
[22] V. Consonni, M. Knelangen, U. Jahn, A. Trampert, L. Geelhaar, H. Riechert, Appl. Phys. Lett. **95**, (2009)
[23] H. Harima, J. Phys.: Condens. Matter **14**, R967 (2002)
[24] W. Limmer, W. Ritter, R. Sauer, B. Mensching, C. Liu, B. Rauschenbach, Appl. Phys. Lett. **72**, (1998)
[25] T. Richter, H. Lüth, R. Meijers, R. Calarco, M. Marso, Nano Lett. **8**, 3056 (2008).

*Corresponding author: f.limbach@fz-juelich.de